The Accuracy of Vegetation Stand Boundaries Derived from Image Segmentation in a Desert Environment

Andrès M. Abeyta and Janet Franklin

Abstract

Line intercept sampling was used to determine if boundaries between desert scrub vegetation stands corresponded with boundaries between regions in an image derived from a segmentation algorithm applied to Thematic Mapper (TM) data for the Anza-Borrego Desert State Park, California. An image segmentation algorithm developed by Woodcock and Harward (1992) was applied to images comprising TM bands 3, 4, and 5, from April 1987, principal components images based on April 1987 and June 1990 imagery, and each with texture added. The Global Positioning System (GPS) was used to determine coordinates of both physiographic (land-form) and vegetation boundaries in the field as they intersected line transects. These boundary locations were then registered to the segmented images. Image region boundaries that fell within ε tolerances (spatial error bounds) of surveyed boundaries were considered accurate. Image region boundaries showed less than 10 percent omission error but about 50 percent commission error when compared with the true locations of vegetation and physiographic boundaries. The use of image principal components and texture in the segmentations did not produce anticipated increases in the correspondence between field-mapped and image-region vegetation boundaries, although there is some suggestion that multidate principal components may be sensitive to vegetation boundaries, and texture to physiographic boundaries.

Introduction

In order to transform raster-based remotely sensed data into thematic polygonal data to be stored in a vector-based GIS, it is necessary to minimize the number of polygons which must be created in the vector form (Lunetta *et al.*, 1991). Image segmentation is a method of generalizing information derived from classification of remotely sensed imagery so that a minimum mapping unit (MMU) larger than a pixel is created. The purpose of image segmentation is "to define regions in the image that correspond to the objects in the ground scene" (i.e., vegetation stands: Woodcock and Harward, 1992), and those regions can then be converted to vector polygons (Gahegan and Flack, 1996). We conducted a study in a desert scrub environment (Anza-Borrego Desert State Park, southeastern California) to determine if segmentation could be used to accurately delineate regions in an image that correspond to vegetation stands at a scale which was consistent with a targeted MMU. Park personnel had estimated that, for resource management purposes, an MMU of 2 hectares would capture significant variation in vegetation patterns (S. Augustine, personal communication). Our study evaluated segment boundary accuracy using a means of field verification that had not previously been applied to the products of automated segmentation.

Woodcock and Harward's (1992) region-growing image segmentation algorithm has previously been applied to forest and chaparral stand delineation (Woodcock and Harward, 1992; Woodcock *et al.*, 1994; Shandley *et al.*, 1996) and to segmentation of a suburban scene (Ryherd and Woodcock, 1996). These applications have mainly focused on vegetation forming a nearly complete canopy. In the arid landscape of the present study, however, there is a complex arrangement of vegetation with a partial canopy. Consequently, surface reflectance as measured in a multispectral image is dominated by the bare soil component and has high spatial variance. This prompted the question: How would the segmentation algorithm perform in this type of spectrally heterogeneous environment? Vegetation reflectance may not contribute enough to the overall signal for boundaries that delineate vegetation stands to be detected in the image. It may be that reflectance from the soil surface results in polygons representing physiographic (land-form or geomorphic) units instead. It has often been noted, however, that vegetation distributions and geomorphology are closely related in arid environments (Lacaze and Lahroui, 1987), and we hypothesized that additional scene information such as spectral texture and multitemporal data could discriminate between the two.

The purpose of this research was to determine if boundaries between desert scrub vegetation stands, located on the terrain using line intercept sampling, corresponded to boundaries between regions in an image derived from a segmentation algorithm applied to Thematic Mapper (TM) data.

Background

Image Segmentation

Segmentation first became a significant remote sensing image processing method in the late 1970s when agricultural inventories strived for increased accuracy. Segmentation (reviewed in Haralick and Shapiro (1985), Pal and Pal (1993), and LeMoigne and Tilton (1995)) incorporates simple spatial characteristics with those that are spectral by dividing a scene into groups of contiguous pixels. Once the image is broken up into regions, each region can be assigned to a theme

Department of Geography, San Diego State University, San Diego, CA 92182-4493 (janet.franklin@sdsu.edu).

A.M. Abeyta is currently with the ERDAS Corporation, 2801 Buford Highway, Suite 300, Atlanta, GA 30329.

Photogrammetric Engineering & Remote Sensing, Vol. 64, No. 1, January 1998, pp. 59–66.

0099-1112/98/6401-0059$3.00/0

(land-cover or vegetation class) using classification based on average characteristics, or on the plurality from a per-pixel classification overlaid on the segmentation (see also Gahegan and Flack (1996)). It would be naive to expect an image segmentation algorithm based solely on spectral and textural pattern recognition (boundary detection or region growing) to delineate image objects that correspond, one-to-one, to the objects of interest (vegetation stands, land-cover polygons), as human-photointerpreted polygons would. Therefore, based on empirical evaluation, almost all region-growing segmentation approaches are designed to "undermerge" (not create excessively large regions). Final merging takes place when the regions are labeled, and some adjacent regions are assigned to the same class.

Our study utilized the region growing segmentation method developed by Woodcock and Harward (1992). A region growing scheme analyzes the spectral and spatial (i.e., texture) properties of pixels and uses these to merge the pixels into homogeneous regions (Mason, 1979). Woodcock and Harward's algorithm was designed to conservatively "grow" regions in an image by controlling a number of parameters, including the rate of pixel merging, the degree of merging, and minimum and maximum region size (Woodcock and Harward, 1992). It uses multiple passes through the data to merge pixels according to the input parameters, with limitations on how many merges are allowed in a single pass. We chose this segmentation algorithm because it was primarily designed for vegetation stand delineation (Woodcock and Harward, 1992). We define a vegetation stand as a contiguous area of the landscape with similar plant composition and structure, and site characteristics (soil type, slope aspect) (Franklin and Woodcock, 1997). A great number of image segmentation algorithms exist (see reviews cited above), and could be evaluated using the methods we describe below. However, our purpose was not to compare algorithms, but to demonstrate the application of the line-intercept sampling method for comparing vegetation stand boundaries recognized in the field to image regions formed by automated segmentation, which, to our knowledge, has not been done before.

Map Assessment

There has been a tremendous increase in the demand for remotely sensed data for spatial database development (Davis and Simonett, 1991; Star *et al.*, 1991). Consequently, groups such as the American Society for Photogrammetry and Remote Sensing (ASPRS) and the National Committee for Digital Cartographic Data Standards (NCDCDS) have been forced to evaluate the accuracy standards by which spatial data are transferred into a GIS (Thapa and Bossler, 1992). In the case of segmented images, it is difficult to make quantitative statements about their accuracy. Object boundaries change depending on whose interpretation is used. The most widely used approach for evaluating a segmented image has been to compare its classification accuracy to a per-pixel classified image by referencing both to a set of point observations or a photointerpreted reference map (Fu and Mui, 1980; Cross *et al.*, 1988; Shandley *et al.*, 1996; Rhyerd and Woodcock, 1996). The resulting error matrices are compared, and the segmented images were shown to be more accurate in each case cited above.

However, error matrices yield a global estimate of thematic classification error, which convolves both boundary location (delineation) and attribute (class label) accuracy (Congalton and Green, 1993). This approach is necessary when polygon objects are used to model continuously varying terrain properties (Goodchild, 1987), as is the case for photointerpreted vegetation stands. Because image segmentation often defines object boundaries in a processing step separate from assigning attribute labels (although frequently based on the same image data), we wished to evaluate the accuracy of boundary placement rather than the thematic accuracy of classified pixels within polygons. And because photointerpreted vegetation stands boundaries can be extremely variable (see Edwards and Lowell, 1996), we used field observations of boundary locations for evaluation.

Skidmore and Turner (1992) proposed the ratio of correctly located boundaries to total boundary length as a measure of the "boundary positional accuracy" (BPA) of a map. Reference data are collected using the line-intercept sampling method they described. If an object boundary falls within an acceptable error band at the intersection with a field transect, then the boundary is found to be correctly mapped. This technique has been applied to a number of forestry related problems, including forest type mapping, forest fuel sampling, and assessment of logging waste (Skidmore and Turner, 1992). In addition, in the present study we also calculated the proportion of field-located (true) boundary positions that had an image segment boundary within the error band as a measure of boundary omission error in the segmentation map. This is a more useful measure of segmentation performance when image boundaries with no corresponding field boundaries (commission error) result from "undermerging" and are expected to disappear during labeling.

The most well known of the boundary positional error models is the epsilon (ε) band which creates a buffer zone of possible true line location around a cartographic line. The delineation of this zone may be visualized as the process of rolling a circle of radius ε along both sides of the line (Chrisman, 1983). This provides a means of representing the degree of locational uncertainty introduced in the raster-to-vector conversion and image classification processes. The significant sources of error (i.e., registration, digitizing, generalization) can be treated independently and summed to estimate the value for ε (Veregin, 1989).

Methods

The main objective of this research was to determine if boundaries between vegetation stands in an arid area corresponded to those determined by an image segmentation algorithm (Woodcock and Harward, 1992), or if, alternatively, segmentation boundaries were more related to soil surface properties characterizing physiographic (land-form) units (e.g., bajada, wash, rocky upland). We also wished to evaluate segmentation boundaries based on different input variables: Thematic Mapper bands 3, 4, and 5; principal components from a multitemporal image; and image texture. The following hypotheses were addressed:

(1)(a) Boundaries between natural vegetation stands in the study area will correspond to boundaries between image regions derived from segmentation.

(1)(b) Alternatively, boundaries between physiographic (land-form) units in the study area will correspond to boundaries between image regions derived from segmentation.

(2) The segmentation of principal components images derived from multitemporal data will improve the correspondence between vegetation stand and image region boundaries over a single-date segmentation.

(3) The incorporation of a texture band into the image data set that is segmented will improve the correspondence between vegetation stand and image region boundaries.

Description of Study Area

Anza-Borrego Desert State Park covers approximately 2400 km^2 in much of eastern San Diego County and parts of Riverside and Imperial Counties (Lindsay and Lindsay, 1985). The climate is arid, with annual precipitation of 127 to 356 mm

TABLE 1. VEGETATION TYPES FOUND IN THE STUDY AREA, ACCORDING TO THE CLASSIFICATION SYSTEM OF SPOLSKY (1979) AND CROSS-REFERENCED TO HOLLAND (1986), A CLASSIFICATION SYSTEM THAT IS LESS DETAILED BUT MORE WIDELY USED. ASTERISKS INDICATE VEGETATION TYPES WITHIN WHICH PLANTS TEND TO HAVE A CLUMPED DISTRIBUTION; OTHER VEGETATION TYPES ARE CHARACTERIZED BY MORE EVENLY DISTRIBUTED PLANTS

Holland (1986)	Spolsky (1979)
30000 Scrub and Chaparral	2.0 Shrub Communities
33100 Sonoran Creosote Bush Scrub	2.4 Sonoran Creosote Bush (*Larrea*) Scrub 2.9 *Larrea-Encelia* scrub
33200 Sonoran Desert Mixed Scrub	
* 33210 Mixed Woody	2.6 Ocotillo fan scrub
33220 Mixed woody/succulent	2.13 *Encelia*-semisucculent scrub 2.14 *Opuntia-Agave* scrub
*	2.15 *Agave* scrub
* 33300 Colorado Desert Wash Scrub	2.19 *Hymenoclea* (cheesebush) wash scrub
60000 Riparian	6.0 Woodland Communities
* 62200 Desert Dry Wash Woodland	6.7 *Psorothamnus* (smoke tree) wash woodland

and summer high temperatures in excess of 38°C. Pacific marine storms create a distinct rainy season (January through March) which is needed to germinate spring flowers (Lindsay and Lindsay, 1985). The park has over 600 species of desert plants. Examples of the major vegetation types characterized by dominant species are listed in Table 1. The study area is approximately 26 km² and is located on the northeast side of State Highway S-2 in the southern end of the park (Figure 1). The geomorphology of the area is characterized by a gently sloping bajada with alluvial fans and washes. This area was chosen for its moderate topography, which accounts for its odd shape because adjacent mountains and badlands were excluded.

Image Data

Anza-Borrego Desert State Park has been imaged by the Landsat TM sensor with a nominal 30-m ground resolution. Images acquired on 24 June 1990 and 13 April 1987 were georeferenced to the California Zone 6 State Plane grid (NAD 27) by STX Inc. Registration was based on a deterministic sensor-Earth geometry model using the Landsat ephemeris data recorded with the TM image. Terrain correction was based on 1:250,000-scale digital elevation models. The 1987 image was purchased after the 1990 image, and the upper left pixel and the ground control points from the 1990 image were used for registration in order to minimize registration error between the two images.

These image dates were chosen in order to explicate the differing phenologies of various vegetation types in the spring and summer. Based on their availability to us, the images that were used were recorded three years apart and field data were collected seven years after the first image. Ideally, imagery and field data from the same calendar year would have been used. However, it was reasoned that their xerophytic characteristics tend to protect the shrub communities from short-term interannual fluctuations in temperature and precipitation. Also, judging from the monthly precipitation totals from the years of data collection, there seemed to be no anomalies that would cause vegetation boundary changes (see Abeyta, 1995). Any slight migration of vegetation boundaries was therefore not taken into account in the error-band distance (see below) which might make the positional accuracies calculated in this study somewhat conservative. The three-month seasonal separation between the two images was deemed adequate to emphasize the phenological contrasts of certain vegetation types. Based on field observation, May and June harbored the most change because ephemeral annual growth dried up quickly during that period.

April was chosen for the single-date image segmentation due to the greater coverage of vegetation in the spring which should reduce the influence of the soil background component in the spectral signature. In addition to a three-band April image comprising the red (Figure 2), near-infrared, and mid-infrared wavelength regions, two other data layers were incorporated into the segmentations. The first layer consisted of principal components based on the covariance matrix from a composite image that was created using TM bands 3, 4, and 5 from both the April and June images. The first four components explained 87, 6, 4, and 2 percent of the variance in the multidate data (99 percent in total) and so were used as input to segmentation. Principal components (PC) analysis is a data compression technique, and while it would have been desirable to use all bands from both dates to calculate PC images, some bands were not available because the archival tape had become corrupted. Consequently, we chose bands 3, 4, and 5 for the single- and multidate analyses because they have been shown to be related to vegetation patterns in arid regions (Franklin, 1991). The June imagery was only used in the principal components analysis. The other variable used was a texture band. A variance-based texture image was created where the digital number of a pixel is the local variance in an adaptively placed 3 by 3 window (Ryherd and Woodcock, 1996). The texture band was created from April band 3 (red) because of its usefulness in discriminating between vegetation and soil, and its prior use in vege-

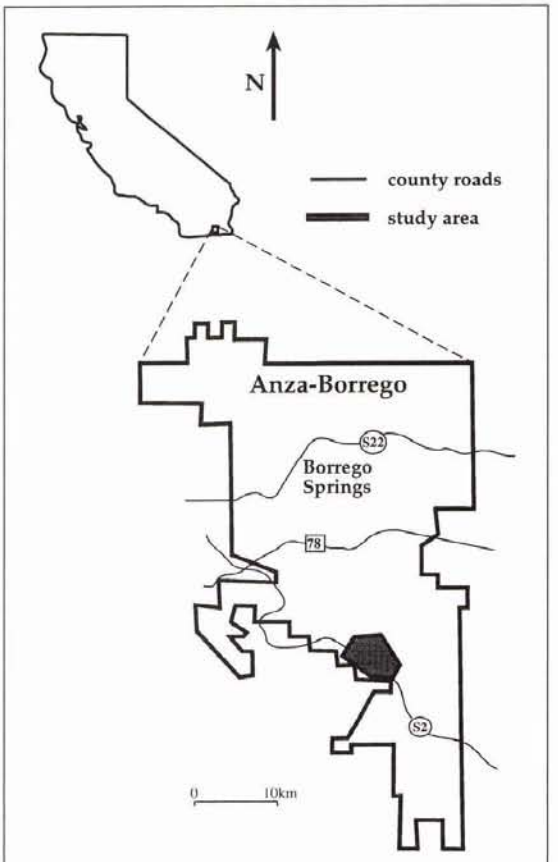

Figure 1. Study area (shaded) located within the Anza-Borrego Desert State Park in southeastern California.

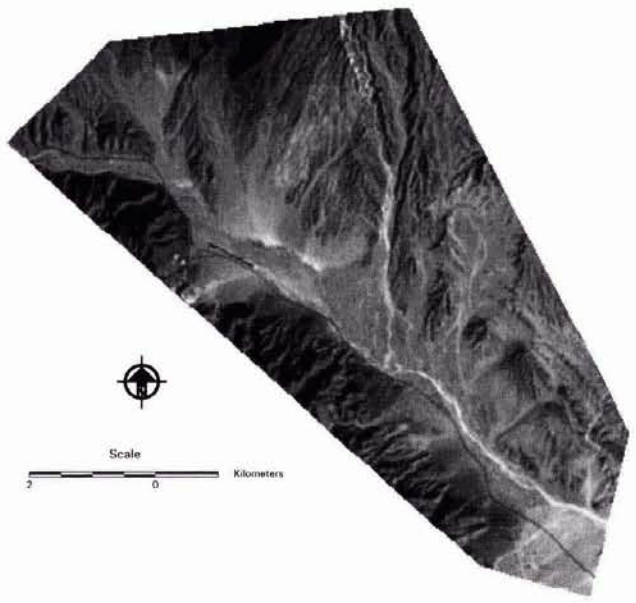

(a)

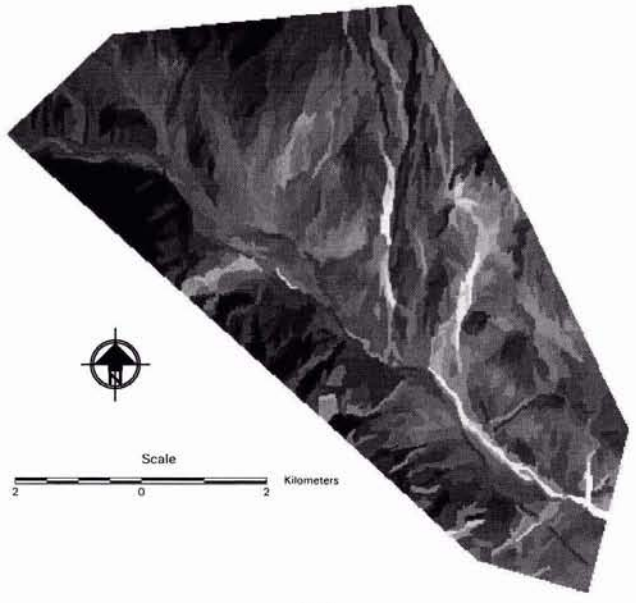

(b)

Figure 2. (a) April 1987 TM Band-3 image, corresponding to the study area delineated in Figure 1. (b) Segmentation resulting from the April three-band image, shown for April Band 3 (where the grey tone of each segment is the average Band-3 grey tone of all pixels falling within the segment).

tation mapping (Franklin *et al.*, 1986; Woodcock *et al.*, 1994).

Image Segmentation

The Woodcock-Harward segmentation algorithm was implemented using the IPW (Image Processing Workbench) software (Frew, 1990). The segmentation parameters used by Shandley *et al.* (1996) served as a reference for determining optimum values for the desert scene. Although many of the parameters values were varied during a sensitivity analysis, minimum region size, maximum region size, and texture scaling were found to be the most influential on segmentation outcomes. After many trials with varying parameters (Abeyta, 1995), a set of revised values was chosen (Table 2).

The global merge tolerance (t) specifies the Euclidean distance in feature space within which adjacent pixels would be allowed to merge (in units of Digital Number based on spectral bands and the other variables which were quantized to one-byte images) and was set at 6. The merging coefficient (m) was set at 0.1 (no more than 10 percent of the regions were merged on each pass). The normal region merge value (*Nnormin*) produces merging in auxiliary passes for those regions with smaller areas than the specified value. Its value was defaulted to the value of the absolute minimum number of pixels parameter (*Nabsmin*). When a texture band was added, a weighting factor of 6 was used (only coincidentally the same number as t). This value proved to be the greatest change from those parameter values used by Shandley *et al.* (1996). Weighting of the input bands in image segmentation will be discussed further below.

In summary, the following input variable combinations were segmented: (1) April band 3, 4, and 5 image; (2) principal components (PCs) 1 through 4 from a six-band multitemporal image; (3) three-band April plus texture; and (4) first-four PCs plus texture.

Line-Intercept Sampling of Boundary Locations

Line-intercept sampling was used to determine the actual locations of vegetation and physiographic boundaries in the field. Pending the selection of "best" segmentation parameters, a segmentation using *Nabsmin* = 20 and *Nmax* = 400 was used to estimate the number of field transects needed. A set of 40 randomly located 0.8-km transects was overlaid on the segmented image which produced an average of 3.3 intersections per transect. It was then necessary to determine the least number of transects needed to assess boundary accuracy at a 95 percent confidence level using the following formulas from Skidmore and Turner (1992):

$$C\hat{V}(\hat{X}) = \sqrt{\frac{n}{t^2}}\,E \qquad (1)$$

where

$C\hat{V}(\hat{X})$ = coefficient of variation of estimated boundary length ($\hat{X}$) of polygons per unit area;
n = estimated number of line transects needed;
t = Student's t statistic at a 95 percent confidence level;
E = prespecified allowable error fraction;

$$m = \left[\frac{1}{C\hat{V}(\hat{X})}\right]^2; \qquad (2)$$

where

TABLE 2. PARAMETER VALUES USED IN WOODCOCK AND HARWARD'S SEGMENTATION ALGORITHM (t IS EUCLIDEAN DISTANCE IN FEATURE SPACE IN DIGITAL NUMBER UNITS: *Nabsmin, Nnormin, Nviable* AND *Nmax* ARE EXPRESSED AS NUMBERS OF PIXELS; m AND s ARE UNITLESS)

Parameter	Value
global merge tolerance t	6
merging coefficient m	0.1
absolute minimum pixels in a region *Nabsmin*	30
minimum region size merging threshold *Nnormin*	30
critical region size *Nviable*	100
maximum region size *Nmax*	100
texture scaling factor s	6

TABLE 3. ITERATIVE TRIALS FOR CALCULATING THE NUMBER OF TRANSECTS NEEDED TO ASSESS BOUNDARY ACCURACY AT THE 95 PERCENT CONFIDENCE LEVEL WHERE n = NUMBER OF LINE TRANSECTS, m = TOTAL NUMBER OF INTERSECTIONS, A = NUMBER OF INTERSECTIONS PER TRANSECT, AND $C\hat{V}(\hat{X})$ IS DESCRIBED IN EQUATION 1

n	$C\hat{V}(\hat{X})$	m	A
9	0.13	59.1	6.6
10	0.14	51.2	5.1
11	0.15	45.1	4.1
12	0.16	40.4	3.4
13	0.17	36.6	2.8

m = number of total intersections of transect lines with polygon boundaries; and

$$A = \frac{m}{n}; \tag{3}$$

where

A = average number of intersections per transect.

A value for n can be found iteratively by first using an estimate of n in Equation 1, setting $E = 0.1$, and using Equations 2 and 3 to calculate an A which can be compared to the A value obtained from a segmented map. Thus, the estimated number of transects should result in an A value less than or equal to the map A value. An estimated 12 transects of length 0.8 km resulted in an $A = 3.4$ (Table 3) which approximates that found on the preliminary segmented image ($A = 3.3$).

GPS-located field boundaries were used to produce a ground reference data set with a locational accuracy of within 5 m (Slonecker and Hewitt, 1991). Field data were collected in April 1994 using the Trimble GPS Pathfinder Professional Unit. Random coordinates were generated for origins of field transects and fieldworkers navigated to them. Then, 0.8-km transects were walked following a randomly chosen constant azimuth. A set of 50 waypoints (individual GPS readings) was recorded at each field boundary encountered and averaged. Notes were taken on the time, boundary type (vegetation or physiographic), approximate coordinates, and biophysical characteristics of areas lying on either side of the boundary.

Boundaries were determined visually (e.g., without quantitative vegetation sampling) but according to the following criteria. Both species composition and density were observed and noted at a scale (grain) of approximately 2 ha to determine the location of vegetation boundaries. A list was made of the dominant shrub species, as they define the vegetation types (Table 1) and would be the most likely to influence spectral response of the surface. Identification of boundary locations was determined to be consistent among different observers.

Trimble's PFINDER software (Trimble Navigation Ltd., 1992) was used to process the GPS data. The averaged and differentially corrected field data were combined into a single file and edited using field notes to separate points falling on vegetation boundaries from those on physiographic boundaries. The two new files were then converted into ARC/INFO (ESRI Inc., 1994) point files.

Each of the segmented images was first converted from an ERDAS.LAN (ERDAS Inc., 1991) image file to an ARC/INFO GRID raster file. A point-to-boundary distance could now be calculated in ARC/INFO (see Figure 3). Using the NEAR command, a file was created that calculated the distance from each field point to the nearest ARC boundary circumscribing a region. The files containing the distances were then exported to spreadsheet software for calculation of accuracy statistics.

Boundary Positional Accuracy Assessment Using Epsilon Error (ε)

We estimated that georeferencing, resolution, and GPS error contribute 15 m (per image date), 15 m, and 5 m of error, respectively, making ε equal to 35 m for single-date datasets and 50 m for two-date PC images. With subpixel registration accuracy estimated from control points, it is still possible that the actual location of a pixel could be misreferenced by half a pixel (15 m). The 15-m resolution error is a consequence of trying to resolve a finite line out of the coarser raster representation of a boundary (Crapper, 1980). The 5-m average GPS error results from the differential correction process (August *et al.* 1994). In effect, a 70- (or 100-) m error band is created around the field boundary within which a mapped boundary could be accurately placed. Distances were calculated in units of feet, because the coordinate system used was State Plane, but will be presented in metric units.

The estimated boundary length of polygons per unit area ($\hat{X}$) is

$$\hat{X} = \frac{\pi m}{2L} \tag{4}$$

where m is the number of intersections between transects and polygon boundaries and L is the total length of transect lines. Skidmore and Turner (1992) give the estimate of BPA as the ratio (X_t) of correct boundary density (where map boundaries coincided with field boundaries), X_r, to estimated total boundary density, X_m: i.e.,

$$X_t = \frac{X_r}{X_m} = \frac{\frac{\pi m_r}{2L}}{\frac{\pi m_m}{2L}} = \frac{m_r}{m_m} \tag{5}$$

where m_r is the number of transect intersections where mapped boundaries correspond to true boundaries, and m_m is the total number of transect intersections with map boundaries. In fact, this is a measure of commission error (what proportion of mapped boundaries have no corresponding real boundary?) and could be referred to as User's BPA. As noted above, in evaluating a segmentation prior to classification, omission errors are more important (what proportion of real boundaries have no corresponding mapped boundary?). Therefore, we also calculated a Producer's BPA, X_p: i.e.,

$$X_p = \frac{m_r}{m_f} \tag{6}$$

where m_f is the total number of transect intersections with true boundaries.

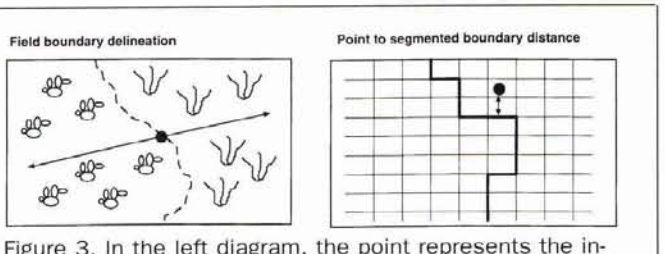

Figure 3. In the left diagram, the point represents the intersection of a vegetation boundary (dashed line) with the line transect (solid line with arrows) — the coordinates of this point are determined with the GPS in the field. The right diagram illustrates a region boundary formed between the pixels comprising two adjacent regions in the segmented image for the same location. Locational accuracy is a function of the average distance from the field points to the nearest segment boundary.

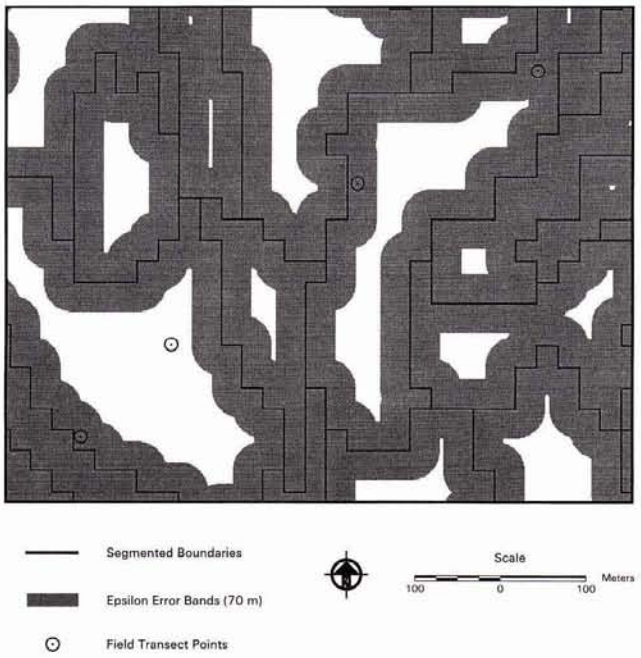

Figure 4. An enlargement of a small portion of the study area showing the polygons resulting from image segmentation (of the April three-band image), and the width of the error bands. Some boundary points (where field transects intersected with vegetation or physiographic boundaries) are shown.

If the boundary density is high (as in an undermerged segmentation), or ε is large, a large proportion of the mapped area will fall within the error bands and high agreement between field and mapped boundaries may occur by chance (Figure 4). This would yield the false conclusion that BPA is high. In order to rule out this conclusion, we did one further accuracy evaluation. The true boundary locations were compared to mapped boundary locations while ε was decreased from 35 to 18.3 m. If a high BPA results from the area covered by the error bands, accuracy should be roughly equal to the proportion of the map covered by the ε-bands. If there is a real correspondence between true and mapped boundary locations, accuracy should be higher than the proportion of the map within the error bands, for a given ε, and should not decrease as rapidly with ε.

Results

Although there are published standards for locational (NCDCDS: see Thapa and Bossler (1992)) and thematic (Anderson *et al.*, 1976) map accuracy, there are no standards for boundary accuracy as it was measured in this study. Error modeling for the integration of remote sensing and GIS is reviewed by Goodchild (1994), but no accuracy standards were given that could be applied here. Skidmore and Turner (1992) showed an example where a User's BPA of 65 percent corresponded to a nonsignificant difference between mapped and true boundary density, and an areal map accuracy of 92.7 percent. We used the standard for thematic accuracy (85 percent) as a guideline for determining acceptable accuracy levels in this study. In comparing the results from different trials, it was not possible to test for significant differences among accuracies because the segmentation trials were not based on independent data sets.

The total number of polygons resulting from segmentation of the 1987 April image (Figure 2b) using the optimum parameters (Table 2) was 828; the average number of pixels in each polygon was 95 (8.6 hectares). The number of map (segmentation) boundaries intersected by the 12 field transects (m_m) was 84, and the numbers of vegetation and physiographic boundaries were 43 and 44, respectively (54 unique locations) (Table 4). This indicates that the 12 transects were adequate for estimating boundary density in the segmented image and the field data sets at the 95 percent confidence level (40 intersections required; Table 3). This occurred because the preliminary segmentation used to estimate the number of transects needed had fewer regions (greater maximum region size) than subsequent segmentations, and coincidentally had about the same boundary density as the field data sets. Based on Producer's BPA, we failed to reject hypotheses 1a and 1b which stated that vegetation and physiographic boundaries will correspond to image segmentation boundaries more than 85 percent of the time. However, User's BPA shows a large proportion of segment boundaries (51 percent) that have no corresponding vegetation or physiographic boundary. Further, a large proportion of the mapped area falls within the ε-bands placed around the segmented region boundaries (Table 5 and Figure 4). Could the large number of true boundary locations that fall within the ε distance of a region boundary do so by chance, owing to the large area covered by the ε-bands?

The proportion of the map within the 35-m ε-bands was 83 percent (Table 5). This was startling when compared with the true field boundary overlay which had a Producer's BPA of 95 percent (vegetation and physiography combined; 54 unique locations). This result would seem to support the notion that so much of the area falls within the ε-bands that many boundary locations may correspond to an image region boundary by chance. However, when the ε distance was decreased from 35 m to 30.5 m (Table 5), the proportion of the map within the ε-bands fell to 76 percent while Producer's BPA remained high at 92 percent. When ε = 18.3 m (Table

TABLE 4. NUMBER OF TRANSECT INTERSECTIONS WHERE TRUE (FIELD) AND MAP (SEGMENTATION) BOUNDARIES COINCIDE (m_r), TOTAL NUMBER OF MAP BOUNDARIES (m_m), TOTAL NUMBER OF TRUE BOUNDARIES (m_f), USER'S (X_t) AND PRODUCER'S (X_p) BOUNDARY POSITIONAL ACCURACY, AND MEAN DISTANCE BETWEEN FIELD AND IMAGE BOUNDARY POINTS (IN METRES) FOR PHYSIOGRAPHIC AND VEGETATION BOUNDARIES, FOR IMAGE SEGMENTATIONS RESULTING FROM DIFFERENT COMBINATIONS OF INPUT VARIABLES

Image Input	Boundary Type	m_r	m_m	m_f	X_t	X_p	Distance (m)
April 3-band	land form	41	84	43	0.49	0.95	14.6
	vegetation	41	84	44	0.49	0.93	15.8
PC 1-4	land form	39	77	43	0.51	0.91	21.6
	vegetation	41	77	44	0.53	0.93	21.3
April+texture	land form	42	85	43	0.49	0.98	15.8
	vegetation	40	85	44	0.47	0.91	17.4
PC+texture	land form	40	79	43	0.51	0.93	14.0
	vegetation	42	79	44	0.53	0.95	15.8

TABLE 5. PRODUCER'S BOUNDARY POSITIONAL ACCURACY (BPA) RESULTING FROM REDUCED ε DISTANCE FOR OVERLAY OF ALL BOUNDARY LOCATIONS (VEGETATION AND PHYSIOGRAPHY COMBINED, n = 54) ONTO SEGMENTATION DERIVED FROM 1987 APRIL TM THREE-BAND IMAGE, AND PROPORTION OF EACH MAP FALLING WITHIN THE ε-BANDS (SEE FIGURE 4)

ε Distance	Area in ε band	Boundary Positional Accuracy
35.0 m	83%	95%
30.5 m	76%	92%
18.5 m	56%	64%

5), these values decreased to 56 percent for the proportion of the map within the ε-bands and 64 percent BPA. While the smaller ε is now affecting it, the Producer's BPA for true boundary locations is still higher than the proportion of the map within the ε-bands. Therefore, the agreement between field and segmentation boundaries seems to reflect more than simply the proportion of the area delineated by ε relative to polygon size. There is an effect of ε on BPA (Figure 4). But ε reflects the true magnitude of locational uncertainty between digital image or map data and locations on the Earth's surface which must be accounted for in locational accuracy assessment and remote sensing-GIS integration.

Principal components 1 through 4 were segmented, and the resulting Producer's BPA was about the same as that calculated for the April three-band input, allowing for the larger error band (Table 4). Therefore, Hypothesis 2 is neither confirmed nor rejected for these data. However, the vegetation boundaries have slightly higher User's and Producer's accuracies than the physiographic boundaries only in the trials involving PC images (Table 4).

The number of polygons created when TM bands 3, 4, and 5 plus texture were segmented was 842, and they had an average size of 93 pixels (8.4 hectares). The PCA plus texture segmentation was very similar, having 870 polygons with an average size of 90 pixels (8.1 hectares). In both cases, the texture band increased the Producer's BPA of the physiographic boundaries by a few percent (Table 4). However, with the addition of texture, the vegetation Producer's accuracies either increased (for the PC image) or decreased slightly (for the April image). Results based on User's accuracy also varied. Therefore, Hypothesis 3 was neither confirmed nor rejected.

Discussion

The Producer's BPA was high for all segmentations (omission errors were low for vegetation and physiographic boundaries). However, there were many segment boundaries intersecting each transect that were undetectable in the field (User's BPA ~50 percent; Table 4). The reliability of the field data collection was confirmed by comparing vegetation boundary locations detected by different observers. The locations were remarkably consistent between observers, and the field methods were felt to be adequate for evaluating the presence of physiographic boundaries, as well as vegetation boundaries for those classes highlighted as "clumped" in Table 1 (see Abeyta (1995) for details).

As expected, there was a strong association between vegetation and physiographic boundaries with a high percentage of them coinciding (63 percent). After completing the sampling, it was felt that only those types of vegetation that exhibited a clumped distribution at the scale of the MMU would be accurately delineated in the field. Segmentation boundaries might be detected in the evenly distributed vegetation types where they are spectrally heterogeneous (due to surface texture, differences in vegetation density, etc.), but no boundary would be detected in the field because the area had the same "average" vegetation composition.

The commission error represented by the low User's BPA might also be explained by illumination differences, spectral differences due to the effects of slope angle and aspect. The study area was originally chosen to minimize extreme variation in relief in order to control for illumination differences, yet it still contained small hills and gullies. A visual comparison between the segmented images and the April image showed that many of the excess segmentation boundaries were a result of slope and aspect changes.

Another possible explanation for the commission error is the nature of the segmentation algorithm used, as discussed previously. This algorithm was designed to be conservative in its merging of regions, and the maximum region size is set as a parameter (Woodcock and Harward, 1992; see Table 2). This will tend to create excessive polygons and thus more boundaries. Adjacent regions can later be merged when they are assigned to the same land-cover category in the labeling process with the common boundary being dissolved. The advantage of this approach is that dissimilar areas never end up in the same segment and higher thematic map accuracy is attained. In this sense, the delineation of boundaries in the segmentation process where none exist is not a serious error, and, in fact, is part of the algorithm's design.

The results based on multi-date PC images are inconclusive because principal components based on the covariance matrix have ordered and highly unequal variance properties, and, therefore, PC 1 would have dominated the segmentation. Stable boundaries of perennial vegetation communities are likely to be expressed in the first principal component of a multidate analysis, and a segmentation based only on the lower-order components 2 to 4 (not shown in this paper) yielded very low boundary accuracy (79 percent Producer's accuracy for vegetation and physiographic boundaries combined; Abeyta, 1995). However, lower-order components are likely to be related to ephemeral vegetation components that differ among the major plant communities. Standardizing or weighting the PC variables, as was done with texture, may have yielded different results. Because the PC images showed some promise in identifying vegetation boundaries, this should be explored further.

Conclusion

The purpose of this study was to determine if vegetation stand boundaries in an arid area corresponded to image region boundaries delineated using the image segmentation algorithm by Woodcock and Harward (1992). Vectorized boundaries from Landsat TM segmented images were overlaid with a vector coverage of field referenced points generated from GPS surveys to determine if they were within an ε distance (35 or 50 m) of observed boundaries as a measure of locational accuracy.

Producer's boundary positional accuracies were greater than 90 percent for all combinations of image input data. The physiographic boundaries tended to be delineated with slightly higher accuracies except in the segmentations derived from a multitemporal Principal Components image, which could be explored further using standardized or weighted PCs. Both an April three-band image and a PC image showed slightly increased accuracy in physiographic boundary delineation when a texture band was added. This suggests that the texture band may be influenced by the soil background rather than the vegetative cover. However, all accuracy differences were very slight. User's BPAs were low (errors of commission were high, ~50 percent) but we did not consider this as important a measure of segmentation accuracy, for reasons explained above.

The study area that was selected was a bajada with little topographic relief. If a mapping scheme were implemented using segmentation for a desert environment, adjustments would be needed to account for other vegetation types and for extreme slope and aspect changes encountered in the mountains and badlands. These conditions would probably lead to even greater "over-segmentation," and efforts would have to concentrate on giving accurate labels to the resulting map polygons. This study served as a first step in evaluating image segmentation for generating mapping units for vegetation and physiography in an arid environment. Despite the coarse resolution of TM data, both vegetation stands and physiographic units can be separated into polygons. This was found to be true within the constraints of locational error allowances for georeferencing, resolution, and GPS. Those locational error sources (resolution, registration) make boundary positional ac-

curacy assessment difficult when boundary locations are derived from raster remotely sensed data.

Acknowledgments

This research was supported, in part, by a Grant-in-Aid from San Diego State University. We would like to thank David McKinsey for invaluable technical support; Scott Augustine and other personnel at California Department of Parks and Recreation and Anza-Borrego Desert State Park for encouraging and advising us; Michael Allen, Thomas Hack, Paul McCullough, Greg Nichols, and Douglas Stow for their help and advice; Curtis Gray and Ellen Hines for assistance with image processing and cartographics; and several geography students who assisted in the field as the temperature soared! We are indebted to two anonymous reviewers for greatly improving the manuscript with their thorough critiques.

References

Abeyta, A.M., 1995. *Assessing the Utility of Image Segmentation in an Arid Environment*, Master's Thesis, Department of Geography, San Diego State University, San Diego, California, 83 p.

Anderson, J.R., E.E. Hardy, J.T. Roach, and R.E. Witmer, 1976. *A Land Use and Land Cover Classification System for Use with Remote Sensor Data*, U.S. Geologic Survey Professional Paper 964, 28 p.

August, P., J. Michaud, C. Labash, and C. Smith, 1994. GPS for environmental applications: Accuracy and precision of locational data, *Photogrammetric Engineering & Remote Sensing*, 60(1):41–45.

Chrisman, N.R., 1983. Epsilon filtering: A technique for automated scale changing, *Technical Papers of the 43rd Annual Meeting of the American Congress on Surveying and Mapping*, pp. 322–331.

Congalton, R.G., and K. Green, 1993. A practical look at the sources of confusion in error matrix generation, *Photogrammetric Engineering & Remote Sensing*, 59(5):641–644.

Crapper, P.F., 1980. Errors incurred in estimating an area of uniform land cover using Landsat, *Photogrammetric Engineering & Remote Sensing*, 46(9):1295–1301.

Cross, A.M., D.C. Mason, and S.J. Dury, 1988. Segmentation of remotely-sensed images by a split-and-merge process, *International Journal of Remote Sensing*, 9(8):1329–1345.

Davis, F.W., and D.S. Simonett, 1991. GIS and remote sensing, *Geographic Information Systems, Vol. 1* (D.J. Maguire, M.F. Goodchild, and D.W. Rhind, editors), Longman, England, pp. 191–213.

Edwards, G., and K.E. Lowell, 1996. Modeling uncertainty in photointerpreted boundaries, *Photogrammetric Engineering & Remote Sensing*, 62(4):377–391.

ERDAS, Inc., 1991. *ERDAS Field Guide, Second Edition*, ERDAS, Inc., Atlanta Georgia.

ERSI, Inc., 1994. *Understanding GIS: The ARC/INFO Method*, Environmental Systems Research Institute, Redlands, California.

Franklin, J., 1991. Land cover stratification using Landsat Thematic Mapper data in Sahelian and Sudanian woodland and wooded grassland, *Journal of Arid Environments*, 20:141–163.

Franklin, J., T.L. Logan, C.E. Woodcock, and A.H. Strahler, 1986. Coniferous forest classification and inventory using Landsat and digital terrain data, *IEEE Transactions on Geoscience and Remote Sensing*, GE-24(1):139–148.

Franklin, J., and C.E. Woodcock, 1997. Multiscale vegetation data for the mountains of Southern California: Spatial and categorical resolution, *Scale in Remote Sensing and GIS* (D.A. Quattrochi and M.F. Goodchild, editors), CRC/Lewis Publishers, Inc., Boca Raton, Florida, pp. 141–168.

Frew, J.E., 1990. *The Image Processing Workbench*, Ph.D. Dissertation, Department of Geography, University of California, Santa Barbara.

Fu, K.S., and J.K. Mui, 1980. A survey on image segmentation, *Pattern Recognition*, 13(1):3–16.

Gahegan, M., and J. Flack, 1996. A model to support the integration of image understanding techniques with GIS, *Photogrammetric Engineering & Remote Sensing*, 62(5):483–490.

Goodchild, M.F., 1987. A model of error for choropleth maps, with applications to geographic information systems, *AutoCarto*, 8:165–174.

———, 1994. Integrating GIS and remote sensing for vegetation analysis and modeling: Methodological issues, *Journal of Vegetation Science*, 5(5):615–626.

Haralick, R.M., and L.G. Shapiro, 1985. Image segmentation techniques, *Computer Vision, Graphics and Image Processing*, 29:100–132.

Holland, R., 1986. *Preliminary Descriptions of the Terrestrial Natural Communities of California*, State of California, the Resources Agency, Department of Fish and Game, Sacramento, California, 156 p.

Lacaze, B., and L. Lahroui, 1987. Télédétection des formations géomorphologiques et de la végétation dans un terretoire du Haut Atlas oriental marocain à partir des données du satellite SPOT, *International Journal of Remote Sensing*, 8(5):751–763.

La Moigne, J., and J.C. Tilton, 1995. Refining image segmentation by integration of edge and region data, *IEEE Transactions on Geoscience and Remote Sensing*, 33(3):605–615.

Lindsay, L., and D. Lindsay, 1985. *The Anza-Borrego Desert Region*, Wilderness Press, Berkeley, California, 179 p.

Lunetta, R.S., R.G. Congalton, L.K. Fenstermaker, J.R. Jensen, K.C. McGwire, and L.R. Tinney, 1991. Remote sensing and geographic information system data integration: Error sources and research issues, *Photogrammetric Engineering & Remote Sensing*, 57(6):677–687.

Mason, D.C., 1979. Segmentation of terrain images using textural and spectral characteristics, *Computers and Digital Techniques*, 2(6): 251–259.

Pal, N.R., and S.K. Pal, 1993. A review of image segmentation techniques, *Pattern Recognition*, 26(9):1277–1294.

Ryherd, S., and C.E. Woodcock, 1996. Combining spectral and texture data in the segmentation of remotely sensed images, *Photogrammetric Engineering & Remote Sensing*, 62:181–194.

Shandley, J., 1993. *Using Image Segmentation to Map Vegetation Stands in the Pine Creek Watershed, Cleveland National Forest*, Master's Thesis, Department of Geography, San Diego State University, San Diego, California, 141 p.

Shandley, J., J. Franklin, and T. White, 1996. Testing the Woodcock-Harward image segmentation algorithm in an area of southern California chaparral and woodland vegetation, *International Journal of Remote Sensing*, 17(5):983–1004.

Skidmore, A.K., and B.J. Turner, 1992. Map accuracy assessment using line intersect sampling, *Photogrammetric Engineering & Remote Sensing*, 58(10):1453–1457.

Slonecker, E.T., and M.J. Hewitt III, 1991. Evaluating locational point accuracy in a GIS environment, *Geo Info Systems*, (June):36–44.

Spolsky, A.M., 1979. *An Overview of the Plant Communities of Anza-Borrego State Park*, unpublished report prepared for Anza-Borrego State Park, Borrego Springs, California.

Star, J.L., J.E. Estes, and F.W. Davis, 1991. Improved integration of remote sensing and geographic information systems: A background to NCGIA Initiative 12, *Photogrammetric Engineering & Remote Sensing*, 57(6):643–645.

Thapa, K., and J. Bossler, 1992. Accuracy of spatial data used in geographic information systems, *Photogrammetric Engineering & Remote Sensing*, 58(6):835–841.

Trimble Navigation Limited, 1992. *GPS Pathfinder User's Manual*, Trimble Navigation Limited, Sunnyvale, California.

Veregin, H., 1989. *A Taxonomy of Error in Spatial Databases*, National Center for Geographic Information and Analysis, Technical Paper 89–12, NCGIA, Santa Barbara, California, 115 p.

Woodcock, C.E., and J. Harward, 1992. Nested-hierarchical scene models and image segmentation, *International Journal of Remote Sensing*, 13(16):3167–3187.

Woodcock, C.E., J.B. Collins, S. Gopal, V.D. Jakabhazy, X. Li, S. Macomber, S. Ryherd, V.J. Harward, J. Levitan, Y. Wu, and R. Warbington, 1994. Mapping forest vegetation using Landsat TM imagery and a canopy reflectance model, *Remote Sensing of Environment*, 50:240–254.

(Received 15 December 1995; revised and accepted 11 March 1997; revised 9 April 1997)